

Ground-state properties of even-even $N = Z$ nuclei within the Hartree–Fock–BCS and Higher Tamm–Dancoff approaches

L. Bonneau¹, P. Quentin², and K. Sieja^{2,3}

¹*Theoretical Division, Los Alamos National Laboratory, Los Alamos, New Mexico 87545, USA*

²*Centre d'Etudes Nucléaires de Bordeaux-Gradignan,*

CNRS-IN2P3 and Université Bordeaux-I, BP 120, 33175 Gradignan, France

³*Institute of Physics, University of M. Curie-Skłodowska, ul. Radziszewskiego 10, 20-031 Lublin, Poland*

(Dated: July 15, 2018)

We calculate the ground-state properties of well deformed, even-even $N = Z$ nuclei in the region between ^{56}Ni and ^{100}Sn within two different approaches, focusing on the binding energy and deformation and pairing properties. First, we employ the Hartree–Fock–BCS (HFBCS) approximation with the Skyrme effective nucleon–nucleon interaction and discuss how the results depend on the parameterization of the interaction and on the pairing force parameters adjusted in various schemes to reproduce the experimental odd–even mass differences. Then, within the Higher Tamm–Dancoff Approximation (HTDA), which explicitly conserves the particle number, we calculate the same properties starting from the HFBCS solutions. The HTDA treatment of the ground-state correlations is converged within a n -particle– n -hole expansion using up to $n=4$ particle-hole excitations of the pair type (in the sense of Cooper pairs). We compare the ground-state properties calculated in these two descriptions of pairing correlations and deduce the importance of the particle-number conservation in weak pairing regimes. Finally, we extend the HTDA calculations so as to include the proton–neutron residual interaction and investigate the role of proton–neutron pairing on the above ground-state properties.

PACS numbers: 21.60.Jz, 21.60.Cs

I. INTRODUCTION

Nuclei with an equal number of neutrons and protons are of a special interest in many respects. The similarity of the neutron and proton single-particle (sp) spin-space wave functions, in the vicinity of the chemical potentials, allows for rather interesting physical studies associated with isospin mixing, β decays and proton–neutron correlations. Such peculiar correlations are encountered in pairing properties either in the $T = 0$ or $T = 1$ channels. Another intriguing property is the so-called Wigner term in a liquid-drop approaches, corresponding to a very sharp pattern of extra stability close to $N = Z$. These nuclei are also of importance for the rapid-proton astrophysical process. Up to $A \sim 60$ for even values of $N = Z$, these nuclei are very close indeed to the proton drip line. However, contrary to the situation near the neutron drip line and due to the Coulomb barrier, their description in a mean-field-plus-correlations approach is not marred by the necessity of dealing accurately with the treatment of the continuum. If one is interested in specific properties of such nuclides and their neighbors (such as the Wigner term), it is desirable to use a description of pairing correlations which is not blurred by fluctuations of the neutron and proton numbers as is the case when using Bogoliubov quasiparticle vacua as ansatz for the ground-state (GS) wave functions.

In this paper we are concerned with the mean-field and beyond-mean-field descriptions of well-deformed even-even $N = Z$ nuclei lying between the doubly magic nuclei ^{56}Ni and ^{100}Sn . To do so we use various Skyrme effec-

tive interactions (SIII [1] and SLy4 [2]) supplemented by two different treatments of the pairing correlations: à la Bogoliubov–Valatin (BCS wave function) and within the particle-number conserving approach dubbed as the Higher Tamm–Dancoff Approximation (HTDA) [3], in both cases for like-particle pairing correlations. Then we add in the latter treatment proton–neutron pairing correlations in $T = 0$ or $T = 1$ isospin channels.

In view of its widespread use for several decades, the BCS approach for like-particle pairing properties is not reviewed here. Only some practical details (among which the choice of the relevant average matrix elements is of paramount importance) are discussed. In contrast the HTDA approach is less widely known and is briefly described here.

The HTDA approach may be presented as a treatment of correlations in a highly truncated shell model whose practicability and efficiency rely on the fast convergence of the particle-hole expansion. This has been shown to be realized upon choosing for the particle-hole quasiparticle vacuum a relevant Hartree–Fock (HF) solution associated self-consistently with the one-body reduced density matrix of the correlated wave function. The HTDA approach was applied for the first time to describe the ground and isomeric states in ^{178}Hf [3] and then odd nuclei and most general isomeric states [4]. A Routhian-HTDA scheme was then proposed to describe the superdeformed yrast bands in the $A \sim 190$ region [5]. A preliminary HTDA study of the GS pairing correlations in ^{64}Ge , including isovector and isoscalar residual interactions, was presented in Ref. [6]. Here the HTDA approach

is applied for the first time in systematic calculations of the properties of medium-mass, proton-rich nuclei.

The outline of the present work is the following. In Sect. II we describe the theoretical background (mostly the HTDA formalism) and explain at length in Sec. III how the calculations are carried out in practice, especially regarding the pairing strength fitting strategy in both BCS and HTDA approaches and the optimization of the harmonic-oscillator basis parameters in the HFBCS calculations. The presentation and discussion of the obtained results is organized in three steps. First, in Sec. IV, we focus on the GS properties obtained within the HFBCS approach, and in Sect. V on the results obtained within the HTDA formalism without proton-neutron coupling in the particle-particle channel. Then we carry out in Sect. VI a comparative study of pairing properties depending on the pairing treatment and the fitting scheme. Finally we extend in Sec. VII the HTDA calculations so as to include the full isovector and isoscalar pairing interaction. The main conclusions of our study are drawn in Sec. VIII.

II. THEORETICAL BACKGROUND

In the HFBCS approach we use the Skyrme effective interaction in the particle-hole channel and the seniority force in the particle-particle channel, and expand the single-particle wave functions in the cylindrical harmonic-oscillator basis, as detailed in Ref. [7].

We focus in the remainder of this section on the HTDA approach. Its purpose is to describe various nucleon correlations (such as pairing and RPA) on the same footing. Among the many particle-hole excitations on a Slater determinant vacuum (noted here $|\Phi_0\rangle^1$), pair excitations around the Fermi surface play an essential role. By construction the HTDA approach is an extension of the Tamm-Dancoff approximation to higher order of particle-hole excitations, so it may be regarded as a truncated shell model. The rapidity of the convergence of the particle-hole expansion, and thus the tractability of the approach, depends on the realistic character of $|\Phi_0\rangle$. A fast convergence is expected to be reached when the quasi-vacuum is defined self-consistently in such a way that some many-body effects of the correlations are already taken into account at the mean-field level.

Let us consider the effective Hamiltonian

$$\hat{H} = \hat{K} + \hat{V}, \quad (1)$$

where \hat{K} denotes the kinetic energy operator and \hat{V} an effective interaction. For the wave function $|\Phi_0\rangle$ we choose

the HF solution, i.e., the eigenstate of the Hamiltonian \hat{H}_{HF} defined by

$$\hat{H}_{\text{HF}} = \hat{K} + \hat{V}_{\text{HF}} \quad (2)$$

where the potential \hat{V}_{HF} denotes the one-body reduction of \hat{V} for $|\Phi_0\rangle$ and is self-consistently obtained from the many-body reduced density matrix $\hat{\rho}$ of the correlated solution $|\Psi\rangle$ for the desired number of particles. We have thus

$$\hat{H}_{\text{HF}}|\Phi_0\rangle = E_0|\Phi_0\rangle, \quad (3)$$

where E_0 is the associated eigenenergy and

$$\hat{H}_{\text{HF}} = \hat{K} + \hat{V}_{\text{HF}}. \quad (4)$$

This approach also allows to include various one-body constraints (on the nuclear deformation for example) in a simple way since the constraint operator can be absorbed in the definition of \hat{H}_{HF} . In addition we assume here that the GS solutions possess the time-reversal, axial and parity symmetries.

The quasi-vacuum $|\Phi_0\rangle$ may now serve to construct an orthonormal many-body basis in which we diagonalize the Hamiltonian \hat{H} . In principle to build this basis we should include, besides $|\Phi_0\rangle = |\Phi_0^\tau\rangle \otimes |\Phi_0^{\tau'}\rangle$, the particle-hole excitations of all orders (from 1 to the particle number) created on $|\Phi_0\rangle$, noted generically $|\Phi_n\rangle$ for n -particle- n -hole (np - nh) excitations. The total GS wave function $|\Psi\rangle = |\Psi^\tau\rangle \otimes |\Psi^{\tau'}\rangle$ can therefore be decomposed in the following way

$$\begin{aligned} |\Psi\rangle = & \chi_{00}|\Phi_0^\tau\rangle \otimes |\Phi_0^{\tau'}\rangle + \sum_{(1p-1h)_\tau} \chi_{10}|\Phi_1^\tau\rangle \otimes |\Phi_0^{\tau'}\rangle \\ & + \sum_{(1p-1h)_{\tau'}} \chi_{01}|\Phi_0^\tau\rangle \otimes |\Phi_1^{\tau'}\rangle + \sum_{\substack{(1p-1h)_\tau \\ (1p-1h)_{\tau'}}} \chi_{11}|\Phi_1^\tau\rangle \otimes |\Phi_1^{\tau'}\rangle \\ & + \sum_{(2p-2h)_\tau} \chi_{20}|\Phi_2^\tau\rangle \otimes |\Phi_0^{\tau'}\rangle + \sum_{(2p-2h)_{\tau'}} \chi_{02}|\Phi_0^\tau\rangle \otimes |\Phi_2^{\tau'}\rangle \\ & + \dots \end{aligned} \quad (5)$$

where τ and τ' denote two different charge states. However practical calculations require to truncate this expansion. Based on the former studies in the HTDA framework [3, 4, 6], we may assume that the components of the pair-excitation type dominate in the GS solution. The set of products of Slater determinants $|\Phi_i^\tau\rangle \otimes |\Phi_i^{\tau'}\rangle$ is an orthonormal basis of the physical space accessible to a nucleus having N neutrons and Z protons. Assuming time-reversal symmetry, the coefficients χ_i in Eq. (5) are real and, if we take $|\Psi\rangle$ normalized to unity, obey the relation

$$\sum_i \chi_i^2 = 1. \quad (6)$$

¹ For the sake of clarity in the notation, we reserve the letter Φ for a Slater determinant and the letter Ψ for a correlated state.

It can be easily shown that the expression (5) of $|\Psi\rangle$ ensures that $|\Psi\rangle$ is an eigenstate of the particle-number operator: $\hat{N}|\Psi\rangle = A|\Psi\rangle$, with $A = N + Z$. Finally, to obtain the correlated ground state we diagonalize the Hamiltonian defined in Eq. (1) in the retained many-body basis.

Now, let us rewrite the Hamiltonian \hat{H} as

$$\hat{H} = \langle \Phi_0 | \hat{H} | \Phi_0 \rangle + \hat{H}_{\text{IQP}} + \hat{V}_{\text{res}}, \quad (7)$$

where the independent quasiparticle Hamiltonian \hat{H}_{IQP} and the residual interaction \hat{V}_{res} are defined by

$$\hat{H}_{\text{IQP}} = \hat{H}_{\text{HF}} - \langle \Phi_0 | \hat{H}_{\text{HF}} | \Phi_0 \rangle, \quad (8)$$

$$\hat{V}_{\text{res}} = \hat{V} - \hat{V}_{\text{HF}} + \langle \Phi_0 | \hat{V} | \Phi_0 \rangle. \quad (9)$$

It is interesting to note that these definitions give a vanishing expectation value of \hat{H}_{IQP} and \hat{V}_{res} for the HF solution $|\Phi_0\rangle$. The independent quasiparticle Hamiltonian can also be expressed as

$$\hat{H}_{\text{IQP}} = \sum_k \xi_k \eta_k^\dagger \eta_k \quad (10)$$

where ξ_k is equal to the energy ϵ_k of the single-particle state $|k\rangle$ if $|k\rangle$ is a particle state with respect to $|\Phi_0^\tau\rangle$ or equal to $-\epsilon_k$ if $|k\rangle$ is a hole state. In Eq. (10), η_k^\dagger is the creation operator a_k^\dagger associated with $|k\rangle$ if $|k\rangle$ is a particle state or the annihilation operator a_k if $|k\rangle$ is a hole state. The matrix element of \hat{H} between two Slater determinants $|\Phi_i\rangle$ and $|\Phi_j\rangle$ of the multi-particle multi-hole basis therefore takes the form

$$\langle \Phi_i | \hat{H} | \Phi_j \rangle = \delta_{ij} (\langle \Phi_0 | \hat{H}_{\text{HF}} | \Phi_0 \rangle + \sum_\tau E_{\text{ph}}^{i(\tau)}) + \langle \Phi_i | \hat{V}_{\text{res}} | \Phi_j \rangle, \quad (11)$$

where $E_{\text{ph}}^{i(\tau)}$ is the particle-hole excitation energy associated with $|\Phi_i^\tau\rangle$ and calculated with respect to the vacuum $|\Phi_0^\tau\rangle$ as

$$E_{\text{ph}}^{i(\tau)} = \sum_{k \in |\Phi_i^\tau\rangle} \xi_k. \quad (12)$$

where the sum runs over all the single-particle states $|k\rangle$ contained in $|\Phi_i^\tau\rangle$. Since the residual interaction contains only one- and two-body operators, the matrix element $\langle \Phi_i | \hat{V}_{\text{res}} | \Phi_j \rangle$ vanishes when $|\Phi_i\rangle$ and $|\Phi_j\rangle$ differ by particle-hole excitations of order three or higher. It can be calculated in terms of two-body matrix elements of \hat{V} by application of the Wick theorem generalized to quasivacua as shown in Ref. [4].

III. CALCULATION PROCEDURE

Since we are in a region of nuclear deformation instability (shape coexistence) our final results can be sensitive

to the choice of the effective interaction and to the pairing treatment. This is why two parameterizations of the phenomenological Skyrme interaction, namely the SIII and SLy4 ones are used. In the particle-particle channel a simple seniority ansatz is adopted in the BCS calculations. It is specified by the value G of the constant pairing matrix elements between any single-particle states in the canonical basis retained in this part of the calculations. The value of G is adjusted to reproduce the so-called empirical pairing gaps evaluated in the 3-point or a 5-point formula [8]. The differences between these two experimentally deduced quantities are large in this region and so are the experimental errors for nuclear masses. In addition the meaning of the pairing gap derived from finite mass differences is no longer clear in the $N = Z$ case. Therefore, we find it necessary to make a comparison of the results obtained in the two cases which represent stronger (5-point fit) and somewhat weaker (3-point fit) pairing regimes. We describe in the next subsection the fitting procedure for G as well as the harmonic-oscillator (HO) basis parameters optimization carried out in the HFBCS framework. The obtained basis parameters are then used in the HTDA calculations assuming that they do not differ significantly from the values that would result from an optimization in the HTDA approach.

Once the solutions corresponding to the equilibrium deformations determined in the HFBCS calculations are found, we perform perturbative HTDA calculations (one diagonalization of the HTDA matrix is performed on top of the HFBCS calculations) without any constraints on the deformation. Since we are interested in the GS correlations of even-even nuclei, the many-body basis includes here only pair excitations, i.e., excitations where nucleons occupying twofold Kramer-degenerate hole levels are scattered into Kramer-degenerate particle levels. As for the residual interaction in the HTDA approach, we choose a δ force whose strength is adjusted as explained in subsection III B. In this way our formalism not only retains the realistic character of self-consistent mean-field calculations, but also ensures the particle number conservation.

A. Pairing strength adjustment in the HFBCS approach

We shall follow here the steps of Bonche and collaborators [9] and apply the BCS approximation with the seniority pairing interaction. For the sake of defining our notation and for completeness, we recall the relevant expressions involved, omitting the isospin τ index. First, the seniority antisymmetrized matrix element is given by

$$\tilde{V}_{k l k' l'} = -G f_k f_{k'} \delta_{l \bar{k}} \delta_{l' \bar{k}'} \quad (13)$$

with the smooth cut-off factor

$$f_k = \frac{1}{1 + \exp[(\epsilon_k - \epsilon_F - \Delta\epsilon)/\mu]} . \quad (14)$$

Here as well as in the HTDA case, the Fermi level ϵ_F is defined by

$$\epsilon_F = \frac{1}{2} (\epsilon_n + \epsilon_{n+1}) \quad (15)$$

where ϵ_n and ϵ_{n+1} denote the energies of the last occupied and the first empty single-particle state, respectively (in a pure HF picture), and $\Delta\epsilon$ and μ denote the cut-off energy and the diffuseness parameters. The pairing gap can be expressed as

$$\Delta_k = f_k \Delta \quad (16)$$

where the state independent gap Δ is given by

$$\Delta = \frac{G}{2} \sum_{k>0} \frac{f_k^2 \Delta}{E_{\text{qp}}^{(k)}} \quad (17)$$

with the quasiparticle energy $E_{\text{qp}}^{(k)}$ defined by

$$E_{\text{qp}}^{(k)} = \sqrt{\tilde{\epsilon}_k^2 + f_k^2 \Delta^2} . \quad (18)$$

In Eq. (17), the sum runs over all the pairs of Kramer degenerate single-particle states, but in fact the cut-off factor f_k suppresses the contributions of single-particle states lying at least about $\Delta\epsilon + \mu$ above the Fermi level. From the average particle number conservation

$$2 \sum_{k>0} v_k^2 = N , \quad (19)$$

we can deduce the expression of the chemical potential λ

$$\lambda = \frac{N - \sum_{k>0} \left(1 - \frac{\epsilon_k}{E_{\text{qp}}^{(k)}}\right)}{\sum_{k>0} \frac{1}{E_{\text{qp}}^{(k)}}} . \quad (20)$$

Finally the pairing energy takes here the simple form

$$E_{\text{pair}} = -\frac{\Delta^2}{G} . \quad (21)$$

We now discuss the determination of the pairing strengths $G_0^{(\tau)}$ related to the actual matrix elements $G^{(\tau)}$ through the following prescription

$$G^{(\tau)} = \frac{G_0^{(\tau)}}{11 + N_\tau} . \quad (22)$$

First we approximately take into account the Coulomb reduction of proton pairing by assuming that, as the

Hartree–Fock–Bogoliubov (HFB) calculations with the Gogny D1S interaction tend to indicate [10]:

$$G_0^{(p)} = 0.9 G_0^{(n)} . \quad (23)$$

Then, for a given parameterization of the Skyrme force and a given set of basis parameters (N_0 , b and q in the notation of Ref. [7]), we determine the GS deformation β_2 of each nucleus using a reasonable initial G -value, assumed to be the same for all the nuclei under study. Then we deduce $G = G_0^{(n)}$ from a least-square fit to the experimental minimal quasiparticle energies through the 3-point and 5-point formulae [8, 11] and using the same single-particle spectrum (the one for the charge state τ corresponding to the converged solution at β_2). We thus have to minimize the following function

$$\chi^2(G) = \frac{1}{2 N_{\text{nucl}}} \sum_{i=1}^{N_{\text{nucl}}} \sum_{\tau=n,p} \left([\mathcal{E}_\tau(G)]_i - [\Delta_\tau^{(\text{exp})}]_i \right)^2 , \quad (24)$$

where \mathcal{E}_τ denotes the lowest quasiparticle energy of the nucleons of type τ and i is an index running over the N_{nucl} nuclei included in the fit. With the obtained G -value, we determine the new GS deformation of each nucleus and minimize again $\chi^2(G)$ to find a new G -value. This procedure is repeated until the simultaneous convergence of G and the GS deformations $\beta_2^{(i)}$ is reached. In practice, it is necessary to scan a wide range of deformations to find the lowest local minimum of the deformation energy curve. The latter is determined using the basis parameters $b = \sqrt{m\omega_0/\hbar}$, with $\omega_0 = (\omega_\perp^2 \omega_z)^{1/3}$, and $q = \omega_\perp/\omega_z$ deduced from an approximate expression for a HO potential (see Ref. [7]). This approximate optimization requires only the knowledge of b_0 , the optimized value of $b(q)$ for a spherical solution. We carry out this study with $b_0 = 0.505$, which is approximately the actual optimal value for the considered nuclei. By varying the basis parameters in the calculated ground states of all nuclei, we have checked that the optimal G -value does not change significantly. The obtained values of G are reported in Table I.

B. Pairing strength adjustment in the HTDA approach

As mentioned earlier, in the HTDA calculations we use a δ force in the particle-particle channel. Both the coupling constant and the cut-off parameter are necessary to define fully the interaction. In our approach it is then necessary to fix the strength of this interaction and this is done by adjusting it so as to reproduce physical quantities for the considered nuclei, e.g., the phenomenological gaps. For that purpose, assuming that the appearance of the pairing gap is related to the breaking of the Cooper pair of lowest energy, we block in the HTDA calculations

TABLE I: Empirical pairing gaps deduced from the odd-even mass differences (using the Atomic Mass Evaluation AME2003 [12]) in 5-point and 3-point formulae [8, 11], except for $\Delta_p^{(5)}$ (^{80}Zr) for which we use the nuclear mass calculated by Möller and Nix [13]. The standard estimate of the pairing gap $12/\sqrt{A}$ is given for comparison. In the last column the experimental binding energy per nucleon is also indicated. All values are in MeV.

Nucleus	$\Delta_n^{(5)}$	$\Delta_p^{(5)}$	$\Delta_n^{(3)}$	$\Delta_p^{(3)}$	$12/\sqrt{A}$	E/A
^{64}Ge	2.07	1.85	1.48	1.14	1.50	8.5294
^{68}Se	2.24	2.01	1.66	1.37	1.45	8.4773
^{72}Kr	1.72	1.73	1.24	1.10	1.41	8.4293
^{76}Sr	1.46	1.635	0.88	1.07	1.37	8.3938
^{80}Zr	1.94	1.57	1.31	0.99	1.34	8.3741

the single-particle level (neutron or proton) closest to the Fermi energy. Then, we adopt the difference between the expectation value of \hat{V}_{res} in a normal (n) and blocked (b) calculations as a proper measure of the pairing correlations that can be compared to the experimental odd-even mass differences. Namely, we define

$$\Delta = (E^{(n)} - E_{\text{IQP}}^{(n)}) - (E^{(b)} - E_{\text{IQP}}^{(b)}), \quad (25)$$

where $E = \langle \Psi | \hat{H} | \Psi \rangle$ and $E_{\text{IQP}} = \langle \Psi | \hat{H}_{\text{IQP}} | \Psi \rangle$.

IV. RESULTS OF THE HARTREE-FOCK-BCS CALCULATIONS

The five selected well-deformed $N = Z$ nuclei are ^{64}Ge , ^{68}Se , ^{72}Kr , ^{76}Sr and ^{80}Zr . For one of the two considered effective interactions (SIII) we use several pairing windows with different values of $\Delta\epsilon$ (6, 8 and 10 MeV) and μ (0.2 and 0.5 MeV). In the fitting process, whereas the choice of $\Delta\epsilon$ is rather unimportant in the considered range, we find that it is not the case for μ . For instance, with $\mu = 0.5$ MeV and $\Delta\epsilon = 6$ MeV, the iterative procedure to adjust of G undergoes oscillations preventing to reach convergence, contrary to all the other pairing windows considered here. We thus retain for further calculations the values $\Delta\epsilon = 6$ MeV and $\mu = 0.2$ MeV stemming as the best choice from the fit to the 5-point experimental gaps. The optimal pairing strengths G_{opt} for the different Skyrme interactions and fitting schemes are displayed in Table II together with the root-mean-square error on the experimental quasiparticle energies σ_{Δ}

$$\sigma_{\Delta} = \sqrt{\chi^2(G_{\text{opt}})}. \quad (26)$$

TABLE II: Optimal G -values and corresponding root-mean-square error on the experimental gaps σ_{Δ} (in MeV) obtained with the SIII and SLy4 Skyrme interactions using the 3-point and the 5-point formulae with $\Delta\epsilon = 6$ MeV, $\mu = 0.2$ MeV and $N_0 = 10$.

Force	Formula	G_{opt}	σ_{Δ}
SIII	3-point	17.7	0.120
SIII	5-point	20.6	0.216
SLy4	3-point	17.2	0.194
SLy4	5-point	19.9	0.260

These adjustments have been performed with a basis size defined by $N_0 = 10$. The same adjustment procedure has also been carried out with a much larger HO basis ($N_0 = 16$) in the illustrative case of the pairing window parameters $\Delta\epsilon = 6$ MeV and $\mu = 0.2$ MeV. The optimal value of G and the associated root-mean-square error turns out to be very close to that obtained with $N_0 = 10$. This justifies the choice of $N_0 = 10$.

It is worth adding that the authors of Ref. [9] performed similar calculations in the same mass region (including for ^{76}Sr and ^{80}Zr) with the SIII Skyrme interaction and the following set of parameters for the seniority force: $\Delta\epsilon = 5$ MeV, $\mu = 0.5$ MeV, $G_0^{(n)} = 13.5$ MeV and $G_0^{(p)} = 16.5$ MeV. The pairing strengths were determined from the experimental quasiparticle energies extracted in the same way as we did from the experimental binding energies.

With the optimal values of the pairing strength of Table II we calculate several GS properties related to the nuclear size (through the root-mean-square mass radius r_m) and deformation (through β_2 and the mass quadrupole Q_{20} and hexadecapole Q_{40} moments), the binding energy per nucleon (E/A) as well as pairing quantities (the BCS pairing gaps Δ_n and Δ_p , the chemical potentials λ_n and λ_p , and the minimal quasiparticle energies \mathcal{E}_n and \mathcal{E}_p). The definitions of β_2 , r_m , Q_{20} and Q_{40} can be found in the Appendix. The obtained results are reported in Table III. The most striking difference between the two Skyrme interactions is that they yield very different GS deformations for ^{80}Zr (strongly prolate with SIII, spherical with SLy4). Moreover the GS deformation of ^{76}Sr drastically depends on the pairing strength when using the SLy4 interaction.

Since the GS deformations calculated with the SIII interaction are in agreement with the experimental data, especially for ^{76}Sr [14] and ^{80}Zr [15], we perform HTDA calculations only with this interaction.

TABLE III: Ground-state properties obtained with the SIII and SLy4 Skyrme interactions and the pairing strengths obtained through the 3-point and the 5-point formulae adjustment procedure. All the quantities in the columns at the right of Q_{40} are expressed in MeV.

Force	Formula	Nucleus	β_2	$r_m(\text{fm})$	$Q_{20}(\text{b})$	$Q_{40}(\text{b}^2)$	E/A	Δ_n	Δ_p	λ_n	λ_p	\mathcal{E}_n	\mathcal{E}_p
SIII	3-point	^{64}Ge	0.200	3.917	2.651	0.0097	8.4216	1.375	1.138	-12.642	-2.713	1.376	1.140
SIII	3-point	^{68}Se	-0.267	4.015	-3.324	0.0535	8.3698	1.173	0.891	-13.040	-2.760	1.502	1.222
SIII	3-point	^{72}Kr	-0.340	4.117	-4.550	0.1038	8.3229	0.966	0.579	-13.057	-2.479	1.299	1.081
SIII	3-point	^{76}Sr	0.390	4.238	7.498	0.2353	8.3024	0.425	0.000	-13.653	-2.584	1.132	0.971
SIII	3-point	^{80}Zr	0.401	4.318	8.441	0.1879	8.2592	0.967	0.623	-13.131	-1.586	1.185	0.965
SIII	5-point	^{64}Ge	0.191	3.918	2.515	0.0141	8.4485	2.035	1.690	-12.775	-2.830	2.036	1.690
SIII	5-point	^{68}Se	-0.244	4.012	-3.062	0.0460	8.3967	2.074	1.709	-13.119	-2.807	2.238	1.876
SIII	5-point	^{72}Kr	-0.259	4.089	-3.546	0.0544	8.3472	2.064	1.710	-13.228	-2.477	2.065	1.712
SIII	5-point	^{76}Sr	0.381	4.234	7.301	0.2133	8.3087	1.380	0.947	-13.537	-2.515	1.683	1.330
SIII	5-point	^{80}Zr	0.384	4.308	8.031	0.1995	8.2741	1.766	1.387	-13.256	-1.685	1.828	1.495
SLy4	3-point	^{64}Ge	0.166	3.887	2.141	0.0010	8.4719	1.162	0.978	-12.687	-2.831	1.162	0.979
SLy4	3-point	^{68}Se	-0.256	3.996	-3.172	0.0344	8.4347	0.672	0.133	-12.984	-2.768	1.551	1.322
SLy4	3-point	^{72}Kr	-0.169	4.047	-2.359	-0.0038	8.3741	1.275	1.058	-13.237	-2.541	1.295	1.075
SLy4	3-point	^{76}Sr	0.392	4.218	7.470	0.2380	8.3402	0.000	0.000	-13.627	-2.597	1.226	1.149
SLy4	3-point	^{80}Zr	0.000	4.158	0.000	0.0000	8.3377	0.461	0.000	-13.911	-2.352	1.458	1.238
SLy4	5-point	^{64}Ge	0.150	3.887	1.922	0.0035	8.4908	1.687	1.426	-12.764	-2.907	1.693	1.430
SLy4	5-point	^{68}Se	-0.228	3.992	-2.844	0.0288	8.4489	1.736	1.376	-13.064	-2.823	2.153	1.837
SLy4	5-point	^{72}Kr	-0.164	4.048	-2.297	-0.0010	8.3958	1.839	1.533	-13.296	-2.608	1.852	1.543
SLy4	5-point	^{76}Sr	0.000	4.097	0.001	0.0000	8.3614	1.805	1.530	-13.952	-2.863	1.867	1.572
SLy4	5-point	^{80}Zr	0.000	4.158	0.000	0.000	8.3450	1.365	1.065	-13.931	-2.383	1.971	1.655

V. RESULTS OF HTDA CALCULATIONS

A. Convergence of the HTDA solutions

In the HTDA calculations two types of truncation schemes need to be defined. The first one is concerned with the maximal order in the many-particle many-hole basis, the second one with the single-particle states from which this basis is built. In the latter case, we are facing thus a situation met in customary BCS calculations. Typically, we limit our single-particle subspace to the configuration-space window defined as

$$|\epsilon_k - \epsilon_F| \leq \Delta\epsilon, \quad (27)$$

where ϵ_F is the Fermi energy and $\Delta\epsilon$ is a cut-off energy. The actual value of $\Delta\epsilon$ is chosen such that single-particle states left out would not contribute significantly except by a renormalization of quantities measuring the intensity of pairing correlations (such as the correlation energy defined below). As already used in HTDA calculations for the ^{64}Ge nucleus [6], we retain here $\Delta\epsilon = 12$ MeV for both charge states. As in the BCS treatment, the two-body matrix elements are multiplied by the smooth cut-off factor of Eq. (14) with $\Delta\epsilon = 12$ MeV and $\mu = 0.2$.

A detailed study of the particle-hole expansion of the HTDA ground state was performed in Ref. [16] in the picket-fence model with 8 or 16 levels filled with 8 or 16 particles, respectively. The authors obtained the convergence of GS solutions toward the exact solution of the Richardson model for a 6p-6h space in the standard nuclear pairing regime. Nevertheless, it may be expected that the realistic character of the HF vacuum calculated with a realistic effective interaction ensures a faster convergence of the particle-hole expansion. This is what the studies of Refs. [3, 6] using a 4p-4h space tend to indicate.

Within the above truncation scheme for the configuration-space window obtained in the HFBCS calculations with the SIII force and $G = 20.6$ MeV, we study the convergence of the HTDA solutions as a function of the many-body basis size. The three quantities under consideration are i) the correlation energy defined as the difference between the expectation values of the Hamilton operator evaluated in the correlated and uncorrelated states

$$E_{\text{corr}} = \langle \Psi | \hat{H} | \Psi \rangle - \langle \Phi_0 | \hat{H} | \Phi_0 \rangle, \quad (28)$$

ii) the occupation probabilities v_i^2 which are defined in the HTDA approach as the diagonal matrix element of

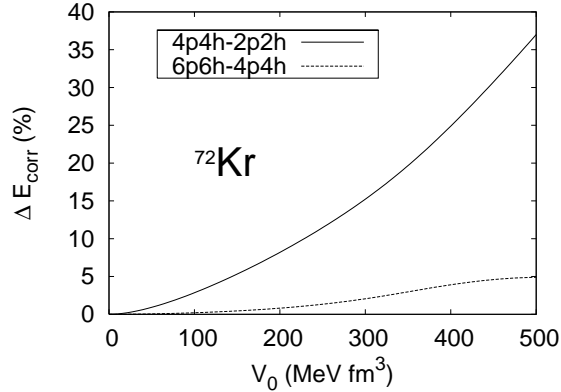


FIG. 1: Convergence of the total correlation energy for ^{72}Kr as a function of the pairing strength V_0 . The percentage difference between correlation energies obtained in many-body spaces that differ by 2p-2h are shown.

the one-body density $\hat{\rho}$ in the single-particle basis

$$v_i^2 = \rho_{ii} = \langle \Psi | a_i^\dagger a_i | \Psi \rangle, \quad (29)$$

where a_i^\dagger and a_i are the creation and annihilation operators associated with the single-particle state $|i\rangle$, respectively, and iii) the mass quadrupole moment (see the Appendix for definitions). Since the one-body density is not diagonal in the HF basis a transformation to the canonical basis is done to obtain the v_i^2 values.

The percentage difference of E_{corr} between solutions obtained in 2p-2h, 4p-4h and 6p-6h spaces of pair excitations are shown for ^{72}Kr as a function of the strength V_0 of the residual δ interaction in Fig. 1. The difference between 2p-2h and 4p-4h solutions is found to be very large and increases nearly linearly with the pairing strength V_0 . The discrepancy between 4p-4h and 6p-6h solutions reaches 5% in the strong pairing region. A similar behavior is found for the other nuclei.

The occupation probabilities of single-particle levels obtained in the different spaces and with different V_0 -values are shown in Fig. 2 for ^{76}Sr . There are no conspicuous differences between the various solutions except in the stronger pairing case, where the difference between the v_i^2 values in 2p-2h and larger spaces becomes substantial. Therefore, the calculated quantities like quadrupole moments and radii converge quickly with the maximal order of particle-hole excitations.

In Tables IV and V, the values of correlation energies and quadrupole moments obtained in 2p-2h, 4p-4h and 6p-6h spaces are given for all nuclei and for two realistic values of the strength of the residual interaction, namely $V_0 = 400 \text{ MeV}\cdot\text{fm}^3$ and $V_0 = 320 \text{ MeV}\cdot\text{fm}^3$ (see the next subsection for details). The largest discrepancy between 4p-4h and 6p-6h results occurs for ^{72}Kr with $V_0 = 400 \text{ MeV}\cdot\text{fm}^3$ where the difference for the correlation energy reaches 3.6%. With the pairing strength

TABLE IV: Correlation energy and mass quadrupole moments obtained in the calculations using 2p-2h, 4p-4h and 6p-6h spaces with the δ -force strength $V_0 = 400 \text{ MeV}\cdot\text{fm}^3$.

Nucleus	$E_{\text{corr}}(\text{MeV})$			$Q_{20}(\text{b})$		
	2p-2h	4p-4h	6p-6h	2p-2h	4p-4h	6p-6h
^{64}Ge	-4.763	-6.383	-6.556	2.670	2.645	2.641
^{68}Se	-4.127	-5.060	-5.205	-3.301	-3.306	-3.306
^{72}Kr	-4.306	-5.348	-5.594	-4.575	-4.528	-4.519
^{76}Sr	-4.010	-4.996	-5.042	7.493	7.482	7.480
^{80}Zr	-4.077	-5.046	-5.228	8.453	8.449	8.448

TABLE V: Same as in Table IV with the strength $V_0 = 320 \text{ MeV}\cdot\text{fm}^3$ of the δ -force.

Nucleus	$E_{\text{corr}}(\text{MeV})$			$Q_{20}(\text{b})$		
	2p-2h	4p-4h	6p-6h	2p-2h	4p-4h	6p-6h
^{64}Ge	-2.992	-3.796	-3.870	2.676	2.656	2.655
^{68}Se	-2.404	-2.798	-2.842	-3.301	-3.304	-3.304
^{72}Kr	-2.558	-2.936	-3.026	-4.595	-4.574	-4.571
^{76}Sr	-2.493	-2.696	-2.758	7.498	7.493	7.493
^{80}Zr	-2.421	-2.768	-2.825	8.456	8.456	8.456

$V_0 = 320 \text{ MeV}\cdot\text{fm}^3$ the discrepancies for E_{corr} amount on the average to 1%. For all five nuclei the differences between the values of the quadrupole moments obtained in 4p-4h and 6p-6h calculations are negligible.

These results suggest that it is reasonable to truncate the particle-hole expansion at order 4. As a matter of fact, this allows for a satisfactory accuracy of the calculations at a rather low cost in terms of computation time. A typical number of many-body configurations to be handled for each charge state is about 5000 while it may rise typically up to 50000 or higher when including 6p-6h excitations. It is worth adding here that in these calculations no additional cut-off on the maximal particle-hole energy of the scattered pairs is applied. The addition of such a cut-off for the particle-hole excitation energy would yield an even faster convergence without losing any substantial accuracy [16] and may be one way to handle calculations of higher particle-hole excitation order.

B. Adjustment of the strength of the residual δ -interaction

The fit of the strength of the δ interaction in the HTDA approach is performed in the space of up to two-pair excitations. Two adjustment schemes are considered: one where the same strength is retained for neutrons (V_{0n}) and protons (V_{0p}), the other one where V_{0p} is reduced by 10% with respect to V_{0n} to account for the Coulomb

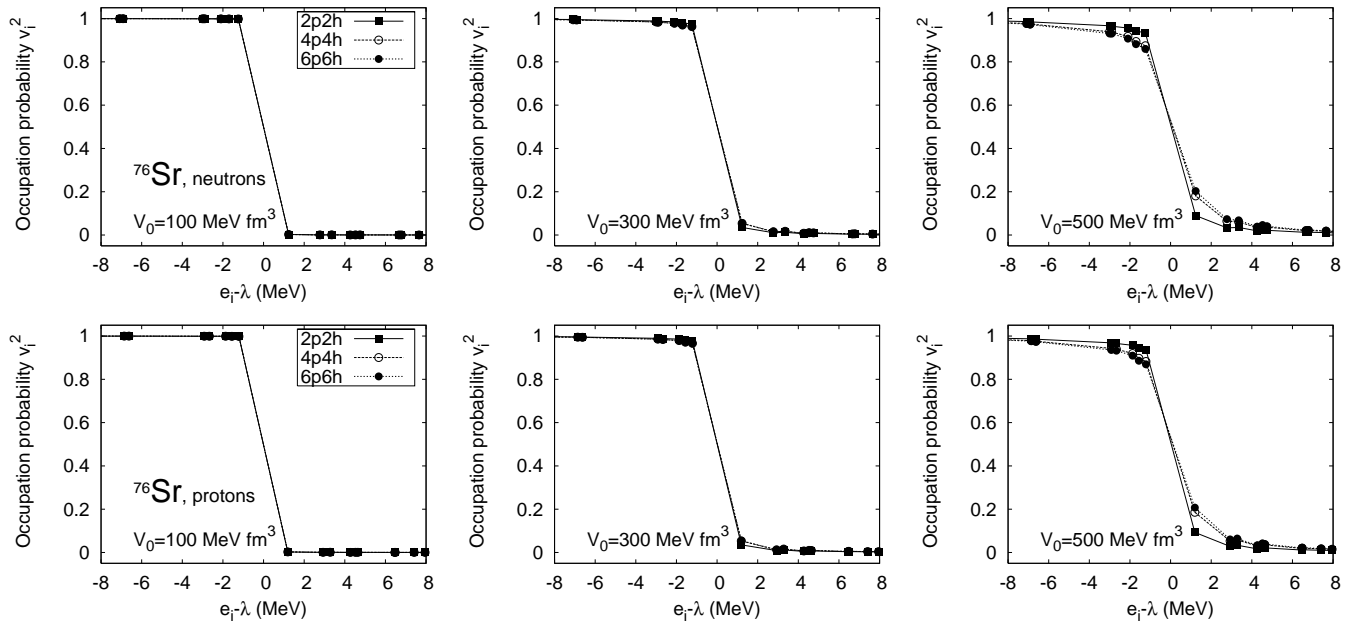


FIG. 2: Convergence of the occupation probability v_i^2 with enlarging of the particle-hole excitations space for neutrons and protons in ^{76}Sr . The cases of three different intensities V_0 of pairing interaction are shown.

anti-pairing effect as in the HFBCS calculations.

In Table VI we present the optimal V_{0p} -values, noted V_0^{opt} , and the associated gap root-mean-square deviations σ_Δ in each adjustment scheme and using the 3-point and 5-point formulae. Since the reduction of V_0^{opt} slightly improves the quality of the fit, we choose this adjustment scheme in further HTDA calculations.

TABLE VI: Optimal values V_0^{opt} (in $\text{MeV}\cdot\text{fm}^3$) and corresponding root-mean-square errors σ_Δ (in MeV) on pairing gaps obtained with the SIII Skyrme interaction using the 3-point and the 5-point formulae.

Formula	$V_{0p} = V_{0n}$		$V_{0p} = 0.9V_{0n}$	
	V_0^{opt}	σ_Δ	V_0^{opt}	σ_Δ
3-point	320	0.278	340	0.264
5-point	400	0.285	420	0.249

C. Ground-state properties obtained within the HTDA approach

As mentioned in Sect. IV, the HTDA calculations use as a starting point the HFBCS solutions obtained with the SIII effective interaction and two sets of values of the pairing-strength adjusted to experimental data through the 3-point and 5-point formulae. The results for the

GS properties are presented in Tables VII and VIII when using the 3-point and 5-point formulae, respectively.

TABLE VII: Ground-state properties within the HTDA framework with the SIII force and the pairing strength obtained through the 3-point formula adjustment procedure. The mass root-mean-square radius r_m , quadrupole moment and hexadecapole moment are given in fm, barns (b) and b^2 , respectively, whereas the binding energy per nucleon E/A and the pairing gaps are expressed in MeV.

Nucleus	β_2	r_m	Q_{20}	Q_{40}	E/A	Δ_n	Δ_p
^{64}Ge	0.201	3.917	2.661	0.0076	8.4340	1.801	1.698
^{68}Se	-0.267	4.014	-3.315	0.0530	8.4004	1.338	1.324
^{72}Kr	-0.341	4.120	-4.575	0.1059	8.3577	1.164	1.152
^{76}Sr	0.389	4.240	7.494	0.2344	8.3344	2.003	1.524
^{80}Zr	0.400	4.320	8.444	0.1830	8.2863	1.216	1.011

Since we are considering here only the equilibrium deformations as determined by the HFBCS calculations, HTDA calculations do not affect much the bulk observables, with the exception of the binding energy and related quantities such as the pairing gaps. The former is indeed much lower (by 2 to 4 MeV) for the HTDA solutions than for the HFBCS ones. Regardless of the adjustment scheme for the pairing strength, the binding energy calculated in the HTDA approach agrees better with the experimental values (see Table I) than in the HFBCS approach.

TABLE VIII: Same as Table VII using the 5-point formula adjustment procedure.

Nucleus	β_2	r_m	Q_{20}	Q_{40}	E/A	Δ_n	Δ_p
^{64}Ge	0.200	3.919	2.651	0.0089	8.4723	2.113	2.011
^{68}Se	-0.266	4.017	-3.318	0.0536	8.4326	2.023	2.006
^{72}Kr	-0.337	4.121	-4.532	0.1027	8.3898	1.718	1.714
^{76}Sr	0.382	4.242	7.483	0.2330	8.3620	2.003	1.524
^{80}Zr	0.400	4.321	8.436	0.1879	8.3138	1.513	1.323

VI. PAIRING PROPERTIES IN BCS AND HTDA APPROACHES

To evaluate the amount of pairing correlations one might think of considering the correlation energy, defined as the difference between the expectation values of the Hamiltonian in the correlated and uncorrelated (HF vacuum) solutions. However, such a correlation energy has no realistic character in practice, in both the HFBCS and HTDA approaches. Indeed, there is no consistency between the interaction used to generate the mean-field and the one building up pairing correlations. Instead, a quantity only related to the residual interaction would be more significant in this respect. This is the case of the so-called condensation energy E_{cond} . In the HFBCS approach, E_{cond} is proportional to the trace of the product of the abnormal density and the pairing field. In the HTDA approach, we may define it by

$$E_{\text{cond}} = E_{\text{corr}} - \sum_i \chi_i^2 E_{\text{p-h}}^i, \quad (30)$$

where the χ_i^2 factors are the probability of the configuration i whose unperturbed particle-hole energy is $E_{\text{p-h}}^i$.

Another variable that may shed light on the amount of pair correlations is the trace of the positive-definite operator $\hat{\rho}^{\frac{1}{2}}(1 - \hat{\rho})^{\frac{1}{2}}$. Indeed, this quantity expresses the non-idempotent character of the density operator $\hat{\rho}$ and is thus related to correlations. As well known in the BCS case, it is related to the abnormal density. Using the occupation factor v_i defined in Eq. (29), we can write the trace of the operator $\hat{\rho}^{\frac{1}{2}}(1 - \hat{\rho})^{\frac{1}{2}}$ simply as the sum $\sum_i u_i v_i$, with $u_i = \sqrt{1 - v_i^2}$.

These two measures of pairing correlations calculated in the HFBCS and HTDA approaches are compared separately for neutrons and protons in Tables IX and X, respectively. The most striking feature is the rather tiny variations in the HTDA case from one nucleus to another. This is due to the resilience of the HTDA solutions to react on variations of the level density at the Fermi surface. In contrast, it is overemphasized in the HFBCS calculations. One example of this is to be found for the protons distribution in ^{76}Sr , where in the HFBCS calculations

TABLE IX: Neutron condensation energies and diffuseness of the neutron Fermi surface obtained in the HFBCS and HTDA approaches. The results with SIII force and two fits of the strength of the pairing interaction are given in each case.

Formula	Nucleus	HFBCS		HTDA	
		E_{cond}	$\sum u_i v_i$	E_{cond}	$\sum u_i v_i$
3-point	^{64}Ge	-4.80	3.4	-5.27	3.2
3-point	^{68}Se	-3.50	3.0	-4.55	2.8
3-point	^{72}Kr	-2.50	2.6	-4.68	2.9
3-point	^{76}Sr	-0.50	1.2	-4.33	2.7
3-point	^{80}Zr	-2.68	2.8	-4.61	3.0
5-point	^{64}Ge	-9.04	4.3	-8.31	3.7
5-point	^{68}Se	-9.95	4.6	-7.85	3.6
5-point	^{72}Kr	-9.78	4.7	-8.16	3.7
5-point	^{76}Sr	-4.53	3.3	-7.70	3.6
5-point	^{80}Zr	-7.75	4.4	-8.20	3.9

TABLE X: Same as in Table IX for protons.

Formula	Nucleus	HFBCS		HTDA	
		E_{cond}	$\sum u_i v_i$	E_{cond}	$\sum u_i v_i$
3-point	^{64}Ge	-3.55	3.1	-3.90	2.9
3-point	^{68}Se	-2.22	2.5	-3.15	2.4
3-point	^{72}Kr	-1.00	1.7	-3.40	2.6
3-point	^{76}Sr	-0.00	0.0	-2.94	2.3
3-point	^{80}Zr	-1.42	2.1	-3.01	2.4
5-point	^{64}Ge	-6.73	3.9	-6.12	3.4
5-point	^{68}Se	-7.34	4.2	-5.58	3.2
5-point	^{72}Kr	-7.46	4.3	-6.11	3.4
5-point	^{76}Sr	-2.36	2.5	-5.33	3.1
5-point	^{80}Zr	-5.70	4.0	-5.48	3.3

with a G -value fitted to the 3-point pairing indicator, no superfluid solution is found (see also Table III for the values of pairing gaps).

VII. PROTON-NEUTRON PAIRING IN THE HTDA APPROACH

In spite of the wide recent theoretical interest paid to the proton-neutron pairing mode, it is still uncertain what is the exact importance of its $T = 0$ component. Moreover, its connection with the Wigner energy is not completely clarified and there are a lot of controversies about other signatures. Since the $T = 0$ pairing is neglected in all fits of the effective interactions in use to

TABLE XI: Ground-state properties of the five considered nuclei as functions of the x value (see text for details).

Formula	Nucleus	r_m (fm)			Q_{20} (b)			Q_{40} (b ²)		
		$x = 0$	$x = 1$	$x = 2$	$x = 0$	$x = 1$	$x = 2$	$x = 0$	$x = 1$	$x = 2$
3-point	⁶⁴ Ge	3.916	3.916	3.917	2.691	2.693	2.697	0.0065	0.0064	0.0062
3-point	⁶⁸ Se	4.012	4.012	4.012	-3.309	-3.308	-3.308	0.0523	0.0522	0.0522
3-point	⁷² Kr	4.119	4.120	4.120	-4.601	-4.602	-4.603	0.1081	0.1082	0.1084
3-point	⁷⁶ Sr	4.239	4.240	4.240	7.499	7.501	7.506	0.2354	0.2356	0.2360
3-point	⁸⁰ Zr	4.320	4.320	4.321	8.446	8.446	8.450	0.1798	0.1795	0.1792
5-point	⁶⁴ Ge	3.917	3.918	3.918	2.688	2.690	2.696	0.0069	0.0067	0.0065
5-point	⁶⁸ Se	4.013	4.013	4.013	-3.308	-3.308	-3.307	0.0525	0.0524	0.0523
5-point	⁷² Kr	4.120	4.120	4.120	-4.590	-4.592	-4.490	0.1073	0.1075	0.1078
5-point	⁷⁶ Sr	4.240	4.240	4.240	7.495	7.498	7.506	0.2351	0.2354	0.2361
5-point	⁸⁰ Zr	4.321	4.321	4.322	8.442	8.444	8.450	0.1811	0.1806	0.1801

calculate the mean-field, this missing contribution may cause some artificial bias in the outcome. In the calculations of masses that make use of a macroscopic energy (liquid-drop models), this problem is circumvented by adding an ad hoc Wigner term. It is however highly predictable that the inclusion of proton-neutron pairing correlations within a HFB approach would lead to novel features of the mean field, as for instance different deformation properties since the usual spin-triplet ($T = 0$) pairing mode would tend to break the axial symmetry. However, since we do not carry out self-consistent HTDA calculations, the mean field itself is not affected by the presence of these proton-neutron correlations.

Expectation values of various observables (such as the radii and quadrupole moments) specifying the correlated wave function have been calculated from solutions obtained after diagonalization of a full isoscalar and isovector residual interaction. For the reasons mentioned in the previous paragraph, these quantities are not expected to change much in this perturbative treatment. In contrast, the change in energy brought in by the consideration of a full $T_z = 0$ part of the interaction is expected to be more significant. In the HTDA framework as applied here, and as far as relative variations are concerned, the correlation energy defined in Eq. (28) is relevant.

The calculations reported in this section are performed in the 4p-4h space of pair excitations containing all new configurations that result from the coupling of neutron and proton states to produce the 0^+ ground state (including aligned proton-neutron pairs). The proton-neutron configurations considerably enlarge the dimension of the Hamiltonian matrices to be computed and diagonalized (up to $\sim 10^5$). As a result, the computing time becomes an issue. This is why we do not test here the convergence of the particle-hole expansion by going up to order 6 as we have done in the previous section. A more detailed study of the proton-neutron pair correlations in the

HTDA approach will be given in a forthcoming publication. In addition, no evidence from previous theoretical approaches has been found for the $T = 0$ collectivity. On the contrary, a rather strong quenching of the isoscalar pairing has been observed in the particular case of pf -shell nuclei. It is thus likely that we only have to deal with a somewhat weak neutron-proton pairing and consequently the 4p-4h limitation should not constitute a stringent constraint.

Based on isospin invariance arguments we choose the strength $V_{0pn}^{T=1} = 1/2(V_{0p}^{T=1} + V_{0n}^{T=1})$ for the part of the residual interaction acting on neutron-proton two-body states. Since the actual $T = 0$ pairing strength is unknown, in other words since one does not know what should be the data pertaining to the determination of a phenomenological such interaction, we adopt an exploratory approach by varying the ratio $x = V_0^{T=0}/V_0^{T=1}$ of the residual interaction in the two isospin channels from 0.5 to 2.0 by steps of 0.5.

In Table XI the resulting GS deformations and radii are indicated only for three values of x , namely 0, 1 and 2. As expected, these quantities do not vary significantly with x .

The relative correlation energy with respect to the $T = 0$ pairing mode, i.e., the difference between the values of E_{corr} calculated with a given x value and with $x = 0$, is plotted in Fig. 3 as a function of x . The correlation energy induced by the $T = 0$ mode is rather important for large x values, so it is highly desirable to get some guidance on the actual value of x . One could argue that the shell-model estimates of Ref. [17] provide a value of about 1.5. However, the shell-model pairing definition with only $(J, T) = (0, 1)$ and $(J, T) = (1, 0)$ couplings is not consistent with the HTDA one where the δ -force in use includes all multipolarities. Therefore, a systematic comparative study of pair correlations in large shell-model calculations and in the HTDA approach would be

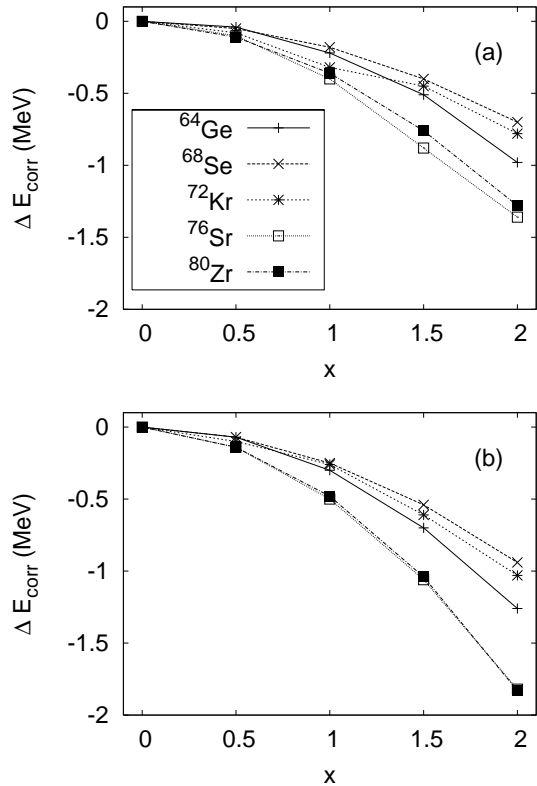


FIG. 3: Correlation energy (in MeV) normalized to the solution without $T = 0$ pair correlations ($x = 0$) as a function of x for all considered nuclei. The case (a), respectively (b), corresponds to calculations with the pairing strength adjusted through the 3-point formula, respectively 5-point formula, in the $T = 1$ channel.

very helpful to better assess a realistic value of x .

Finally it is important to add that the energy shift due to the $T = 0$ pair correlations depends on the pairing intensity in the $T = 1$ channel. Indeed these pair correlations are larger when the $T = 1$ pairing interaction is stronger. This suggests that, in a full treatment of these correlations, the adjustment of the pairing parameters in the $T = 1$ channel should be done with proton-neutron correlations.

VIII. CONCLUSIONS AND PERSPECTIVES

The purpose of this paper is to provide a firm basis to study the correlations present in deformed even-even $N = Z$ nuclei in the $A \sim 70$ region. We mean, first of all, pairing correlations in the sense of Cooper pair excitation of nucleons belonging to similar orbits. For these particular nuclei, proton-neutron correlations must clearly be included in the scheme. Moreover, RPA correlations should be further added. In view of the difficulties to be overcome in achieving this program, we have under-

taken here initial steps by including only proton-neutron pairing correlations in an exploratory way.

Since the various traditional pairing schemes often lead to a weak coupling regime, the Bogoliubov vacuum ansatz for the correlated ground state is rather inadequate. This is especially true for the not-so-heavy nuclei considered here. In contrast the HTDA framework represents a consistent and more physical way of handling various kinds of correlations, including RPA correlations, on the same footing. In the present work, we have chosen to use it from as good as possible HFBCS solutions with the usual pairing treatment which involves the $T = 1$ channel only.

We have had, therefore, to carefully study the pairing channel which includes in particular the choice of a δ interaction strength consistent with the data on atomic masses in the studied region. As a result, we have calculated some deformation properties which are naturally of paramount importance to grasp the single-particle spectroscopic properties. Upon determining the HTDA correlated ground state, we have shown that the diffuseness of the Fermi surface is somewhat similar to what HFBCS yields but less sensitive to the fluctuations of the level density as a function of the mass number.

In the last step, where the full $T_z = 0$ residual interaction has been considered, we have established the feasibility of such calculations. Then, we have assessed in a quantitative way how much the relative amount of $T = 0$ and $T = 1$ components of the residual interaction influences the correlations properties. Even though in this study the $T = 1$ interaction strength is the one adjusted in the absence of a $T_z = 0$ component, it clearly appears from our results that a determination of the above ratio of isospin components is badly needed.

The directions of improvement are therefore easy to perceive. First they imply a better understanding of the residual interaction. Then, RPA correlations should be included in a consistent way, which is currently in progress.

ACKNOWLEDGEMENTS

This work has benefited from the support by the U.S. Department of Energy under contract W-7405-ENG-36, from a funding obtained within the Polish-French (IN2P3) laboratories agreement and from a fellowship of the French Embassy at Warsaw to support the co-sponsored thesis work of one of us (K.S.). These organizations are gratefully acknowledged.

APPENDIX: SPECIFIC QUANTITIES USED TO ASSESS THE DEFORMATION PROPERTIES OF OUR SOLUTIONS

In the HFBCS case, the expectation value of a local one-body operator may be expressed as a space integral

involving the local (diagonal in \vec{r}) one-body reduced density matrix. For the mass or isoscalar (neutron plus proton) distribution, one defines the root-mean-square radius r_m and the quadrupole Q_{20} and hexadecapole Q_{40} moments as

$$r_m = \sqrt{\frac{\int d^3\mathbf{r} \rho(\mathbf{r}) \mathbf{r}^2}{A}}, \quad (31)$$

$$Q_{20} = \int d^3\mathbf{r} \rho(\mathbf{r}) (2z^2 - x^2 - y^2), \quad (32)$$

$$Q_{40} = \int d^3\mathbf{r} \rho(\mathbf{r}) r^4 Y_4^0(\theta), \quad (33)$$

where Y_ℓ^0 denotes the spherical harmonic of order ℓ and magnetic quantum number 0.

We then consider the equivalent spheroid which has the same root-mean-square radius and quadrupole moment as the actual nucleus. Denoting the semi-axes along the symmetry axis and perpendicular to it by a and c , respectively, we have

$$A r_m^2 = \frac{1}{5} (2a^2 + c^2), \quad (34)$$

$$Q_{20} = \frac{2}{5} A (c^2 - a^2). \quad (35)$$

The β_2 parameter is then calculated for this equivalent spheroid by expanding the nuclear radius in polar coordinates according to the β_l -parameterization [13]

$$R(\theta) = \frac{a}{\sqrt{1 - \alpha \cos^2 \theta}} \quad (36)$$

$$= R_0 \left(1 + \sum_{l=1}^{\infty} \beta_l Y_l^0(\theta) \right), \quad (37)$$

with

$$\alpha = 1 - \frac{a^2}{c^2}. \quad (38)$$

This allows us to calculate analytically the expression of β_2 for the equivalent spheroid as a function of α as

$$\beta_2 = \begin{cases} \sqrt{5\pi} \left[\frac{3}{2\alpha} \left(1 - \frac{\sqrt{\alpha(1-\alpha)}}{\text{Arcsin} \sqrt{\alpha}} \right) - 1 \right] & \alpha \in]0; 1[\\ 0 & \alpha = 0 \\ \sqrt{5\pi} \left[\frac{3}{2\alpha} \left(1 - \frac{\sqrt{-\alpha(1-\alpha)}}{\ln(\sqrt{-\alpha} + \sqrt{1-\alpha})} \right) - 1 \right] & \alpha < 0 \end{cases}. \quad (39)$$

In the HTDA case, the above quantities have to be evaluated in the correlated state $|\Psi\rangle$ and one cannot use anymore the usual generalized Wick theorem. Indeed, one has to evaluate matrix elements between two Slater determinants, generally different. One might keep, however, the Wick theorem framework by using mixed densities à la Löwdin [18]. Instead, here we reduce these many-body matrix elements into matrix elements evaluated between single-particle states, which makes the HTDA calculation of the above expectation values similar to the HFBCS ones.

-
- [1] M. Beiner, H. Flocard, N. Van Giai and P. Quentin, Nucl. Phys. **A238**, 29 (1975).
- [2] E. Chabanat, P. Bonche, P. Haensel, J. Meyer and R. Schaeffer, Nucl. Phys. **A635**, 231 (1998).
- [3] N. Pillet, P. Quentin and J. Libert, Nucl. Phys. **A697**, 141 (2002).
- [4] T. L. Ha, PhD thesis, Universite Bordeaux 1 (unpublished).
- [5] P. Quentin, H. Laftchiev, D. Samsøen, I. N. Mikhailov and J. Libert, Nucl. Phys. **A734**, 477 (2004).
- [6] K. Sieja, T. L. Ha, P. Quentin and A. Baran, Int. J. Mod. Phys. **E16**, 289 (2007).
- [7] H. Flocard, P. Quentin, A. K. Kerman and D. Vautherin, Nucl. Phys. **A203**, 433 (1973).
- [8] D. G. Madland and J. R. Nix, Nucl. Phys. **A476**, 1 (1988).
- [9] P. Bonche, H. Flocard, P.-H. Heenen, S. J. Krieger and M. S. Weiss, Nucl. Phys. **A443**, 39 (1985).
- [10] M. Anguiano, J. L. Egido and L. M. Robledo, Nucl. Phys. **A683**, 227 (2001).
- [11] J. Dobaczewski, P. Magierski, W. Nazarewicz, W. Satula and Z. Szymański, Phys. Rev. C **63**, 024308 (2001).
- [12] G. Audi, O. Bersillon, J. Blachot and A. H. Wapstra, Nucl. Phys. **A729**, 3 (2003).
- [13] P. Möller, J. R. Nix, W. D. Myers and W. J. Swiatecki, At. Data and Nucl. Data Tables **59**, 185 (1995).
- [14] E. Náchter, A. Algora, B. Rubio, J. L. Taín, D. Cano-Ott, S. Courtin, Ph. Dessagne, F. Maréchal, Ch. Miehe, E. Poirier, M. J. G. Borge, D. Escrig, A. Jungclaus, P. Sarriguren, O. Tengblad, W. Gelletly, L. M. Fraile and G. Le Scornet, Phys. Rev. Lett. **92**, 232501 (2004).
- [15] C. J. Lister, M. Campbell, A. A. Chishti, W. Gelletly, L. Goettig, R. Moscrop, B. J. Varley, A. N. James, T. Morrison, H. G. Price, J. Simpson, K. Connel and O. Skeppstedt, Phys. Rev. Lett. **59**, 1270 (2001).
- [16] N. Pillet, N. Sandulescu, N. Van Giai and J.-F. Berger, Phys. Rev. C **71**, 044306 (2005).
- [17] M. Dufour and A. P. Zuker, Phys. Rev. C **54**, 1641 (1996).
- [18] P.-O. Löwdin, Phys. Rev. **97**, 1509 (1955).